Unlocking soybean meal pectin recalcitrance using a multi-enzyme cocktail approach

Lauriane Plouhinec, Liang Zhang, Alexandre Pillon, Mireille Haon, Sacha Grisel, David Navarro, Ian Black, Virginie Neugnot, Parastoo Azadi, Breeanna Urbanowicz, et al.

scientific reports

Check for updates

OPEN

Unlocking soybean meal pectin recalcitrance using a multi-enzyme cocktail approach

Lauriane Plouhinec[1,2], Liang Zhang[3,4], Alexandre Pillon[1,5], Mireille Haon[1,5], Sacha Grisel[1,5], David Navarro[1,6], Ian Black[3,7], Virginie Neugnot[2], Parastoo Azadi[3,7], Breeanna Urbanowicz[3,4], Jean-Guy Berrin[1]✉ & Mickael Lafond[1]✉

Pectin is a complex plant heteropolysaccharide whose structure and function differ depending on its source. In animal feed, breaking down pectin is essential, as its presence increases feed viscosity and reduces nutrient absorption. Soybean meal, a protein-rich poultry feed ingredient, contains significant amounts of pectin, the structure of which remains unclear. Consequently, the enzyme activities required to degrade soybean meal pectin and how they interact are still open questions. In this study, we produced 15 recombinant fungal carbohydrate-active enzymes (CAZymes) identified from fungal secretomes acting on pectin. After observing that these enzymes were not active on soybean meal pectin when used alone, we developed a semi-miniaturized method to evaluate their effect as multi-activity cocktails. We designed and tested 12 enzyme pools, containing up to 15 different CAZymes, using several hydrolysis markers. Thanks to our multiactivity enzymatic approach combined with a Pearson correlation matrix, we identified 10 fungal CAZymes efficient on soybean meal pectin, 9 of which originate from *Talaromyces versatilis*. Based on enzyme specificity and linkage analysis, we propose a structural model for soybean meal pectin. Our findings underscore the importance of combining CAZymes to improve the degradation of agricultural co-products.

Keywords Multi-activity enzymatic cocktails, Filamentous fungi, Soybean meal pectin, CAZymes, Rhamnogalacturonan, Animal feed

Abbreviations

AG	Arabinogalactan
AIR	Alcohol insoluble residue
CAZymes	Carbohydrate-active enzymes
CE	Carbohydrate esterase
DNS	3,5-dinitrosalicylic acid
GH	Glycoside hydrolase
HG	Homogalacturonan
HMP	Highly methylated pectin
RDM	Residual dry matter
PMAA	Partially methylated alditol acetate
PGA	Polygalacturonic acid
PL	Polysaccharide lyase
SBM	Soybean meal
RG	Rhamnogalacturonan
XG	Xylogalacturonan

[1]BBF, Biodiversité et Biotechnologie Fongiques, INRAE, Aix-Marseille Univ, Marseille, France. [2]Adisseo France S.A.S, CINAbio, Toulouse, France. [3]Complex Carbohydrate Research Center, University of Georgia, Athens, GA 30602, USA. [4]Department of Biochemistry and Molecular Biology, University of Georgia, Athens, GA 30602, USA. [5]INRAE, Aix-Marseille Univ, 3PE Platform, Marseille, France. [6]INRAE, Aix Marseille Univ, CIRM-CF, Centre International des Ressources Microbiennes- Champignons Filamenteux, Marseille, France. [7]DOE Center for Plant and Microbial Complex Carbohydrates, University of Georgia, Athens, GA 30602, USA. ✉email: jean-guy.berrin@inrae.fr; michael.lafond@univ-amu.fr

Pectin is a complex heteropolysaccharide forming part of the plant cell wall alongside cellulose and hemicelluloses[1,2]. Its composition and structure depend on many parameters, such as plant origin and growth stage[3], making it one of the most recalcitrant polysaccharides in the plant kingdom[4]. The pectin backbone consists of D-galacturonic acid (D-Gal*A*) linked in α-(1,4), often modified by methyl-ester and/or acetyl-ester substituents[5,6]. While linear pectin is called homogalacturonan (HG), xylogalacturonan (XG) corresponds to the xylosylated form of HG, where D-Gal*A* residues are substituted by D-xylose linked in β-(1,3)[7,8]. Rhamnogalacturonans of types I (RG-I) and II (RG-II) are branched pectin fragments. The backbone of RG-I is composed of D-Gal*A* and L-rhamnose (L-Rha) residues alternatively linked in α-(1,4) and α-(1,2). The L-Rha residues are branched by α-(1,5) arabinans, β-(1,4) galactans[9,10], and arabinogalactans (AG) of types I and II[11]. AG-I consists of β-(1,4)-galactans, which are branched through α-(1,3) linkages with α-(1,5)-arabinans. These arabinans can in turn be substituted by α-(1,2) and/or α-(1,3)-arabinofuranosyl residues[12]. In contrast, AG-II is composed of β-(1,3)-galactans, which are substituted by β-(1,6)-galactans. The terminal ends of these structures can be further decorated by L-arabinose, D-glucuronic acid (D-Glc*A*) or L-fucose[13,14]. RG-I side chains can be further linked to each other through di-ferulic bridges[15] and a recent study revealed that RG-I is covalently bound to AG proteins in the cell wall of *Arabidopsis*[16]. On the other hand, side chains of RG-II are highly complex pectic domains composed of more than 20 different glycosidic bonds and up to 13 neutral and charged sugar residues[17].

Due to its structural complexity, the deconstruction of pectin requires the action of multiple enzymes, classified as carbohydrate-active enzymes (CAZymes)[18]. The CAZy database references catalytic modules capable of creating, modifying or degrading glycosidic bonds, as well as accessory carbohydrate-binding modules, all divided into six classes and 513 families (December 2024; www.cazy.org). In nature, filamentous fungi are efficient degraders of plant biomass as they possess a broad enzymatic arsenal for the breakdown of complex polysaccharides[19,20]. Many fungal enzymatic cocktails containing CAZymes have been developed for biotechnological purposes, ranging from uses in biorefineries to the animal feed industry[21–23]. One such example is the Rovabio™ Advance, an enzyme cocktail produced by the fermentation of *Talaromyces versatilis* and commercialized by the Adisseo® company for the feed industry[24]. Previous studies have reported the use of *Talaromyces* sp. strains for the degradation of pectin-rich substrates[25–27] and others described the use of *Aspergillus terreus* for pectinase production[28–30]. While emphasis is often placed on fungal secretomes, only scarce studies have examined the interplays involved in pectin hydrolysis by fungal enzymes[31,32]. Through a time-course analysis of *A. terreus* secretomes, we recently demonstrated the crucial role of pectin-degrading enzymes in breaking down soybean meal (SBM), a protein-rich substrate widely used in animal feed[33]. Additionally, we highlighted the beneficial effect of supplementing the Rovabio™ Advance with these secretomes to enhance SBM digestibility and protein solubilization. Given its viscosity, SBM pectin can limit access to proteins and amino acids in the animal gut, underscoring the need to better understand its structure and the enzymes required for its breakdown, which remain poorly characterized[34].

Building on this knowledge, the present study aims to deepen our understanding of the pectinolytic enzyme repertoire of *A. terreus* and *T. versatilis*. We selected and recombinantly produced 15 fungal CAZymes putatively active on pectin. After validating their activity and specificity towards pectic substrates, including soybean RG-I, we developed a semi-miniaturized method to investigate their interplay on SBM. By designing 12 enzymatic pools and evaluating their functionality against various hydrolysis markers, we highlight the effectiveness of *T. versatilis* CAZymes on SBM pectin. Finally, integrating our findings with a GC-MS linkage analysis of the pectin fraction from SBM, we propose a simplified model of SBM pectin structure.

Results

Selection and recombinant production of a set of 15 putative pectinolytic enzymes

Fifteen putative pectin-degrading enzymes were selected for recombinant production based on time-course secretomic analyses of *A. terreus*[33], and *T. versatilis* (Supplementary Figure S1). To identify these enzymes, our focus was made on CAZymes highly secreted during the culture of the two fungal strains on pectin-rich substrates and on CAZy families that are poorly represented in the Rovabio™ Advance (Supplementary Figure S1). All produced enzymes belong to three distinct CAZy classes: Carbohydrate Esterases (CEs), Glycoside Hydrolases (GHs), and Polysaccharide Lyases (PLs). Except for GH79 enzymes, the selected GHs exhibited high production levels in *Pichia pastoris*, reaching up to 189 mg of protein per liter of inducing medium for *Tv*GH93 (Supplementary Table S1). Even though *At*PL1_4 displayed a lower production, all recombinant enzymes were sufficiently expressed for further analysis.

From a structural point of view, most of the CAZymes selected consist of a single module corresponding to the catalytic domain (Fig. 1). Two exceptions are the bimodular enzymes *Tv*CE8-GH28 and *At*GH79-GH78, displaying two independent catalytic modules. The first one features a CE8 pectin methyl esterase N-terminal domain and a GH28 polygalacturonase C-terminal domain connected by an 86 amino-acid linker rich in serine and threonine. The bimodular enzyme and the two individual domains were successfully produced in *P. pastoris*. However, regarding the bimodular enzyme *At*GH79-GH78, only the N-terminal GH79 module (referred to as *At*GH79) was successfully expressed, despite multiple attempts to produce it in its full-length form.

Activity determination of the recombinant pectinolytic CAZymes

Enzyme activity was determined using a library of 36 plant-derived and synthetic substrates (Fig. 2). Overall, most enzymes display a substrate specificity in agreement with the activity described in the CAZy families they belong to. As an example, all recombinant GH28 enzymes are active on polygalacturonic acid and oligogalacturonides, but they exhibit a decreased activity on methylated pectin. Similarly, *At*GH29 is active on pNP-α-fucose, confirming its α-fucosidase activity. While both GH78 enzymes (*At*GH78b and *Tv*GH78) are active on pNP-α-rhamnose, only a weak activity is observed on soybean RG-I using the reducing sugar assay,

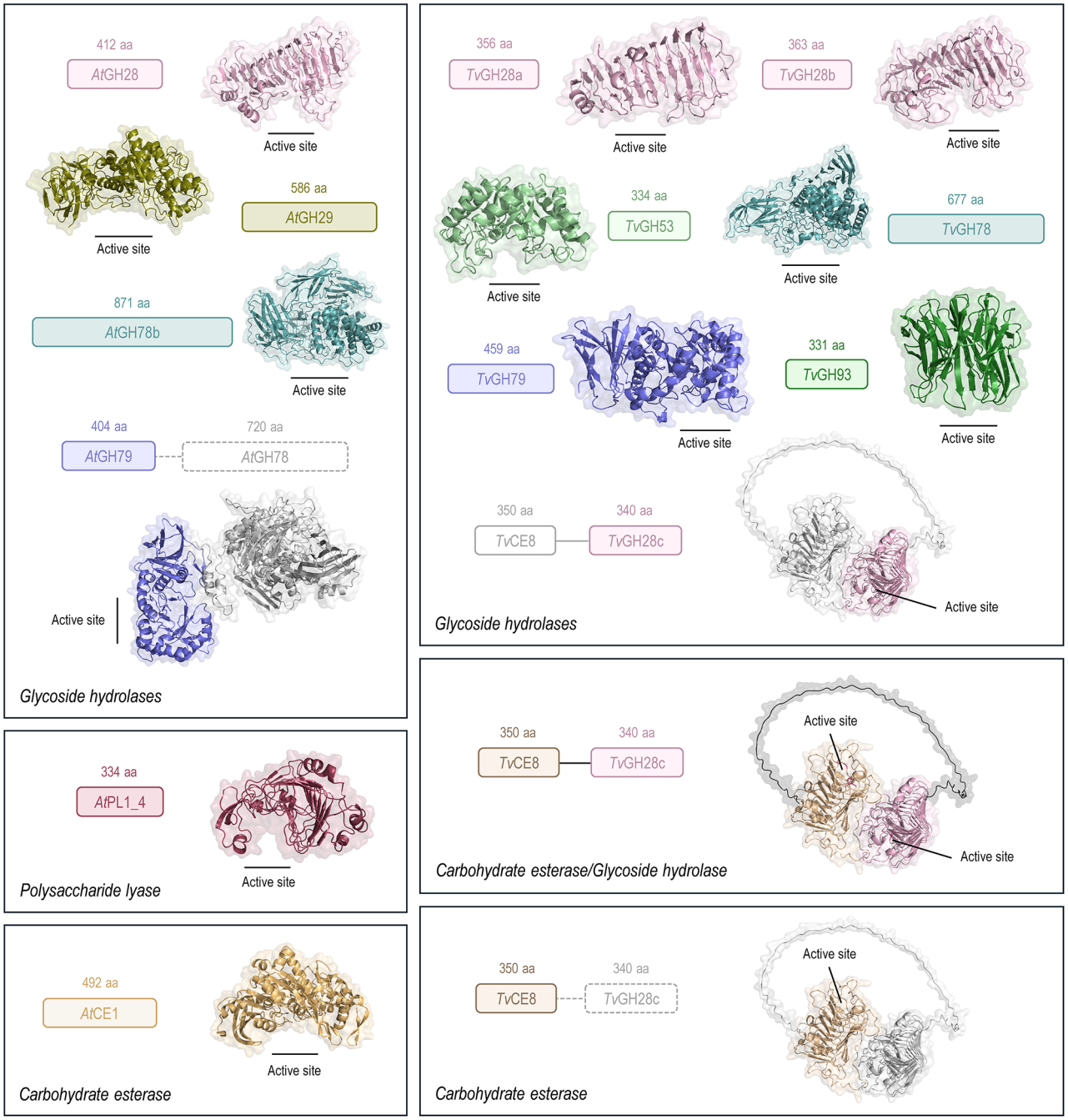

Fig. 1. Modular and structural features of the putative pectinolytic enzymes used in this study. Enzyme active sites are indicated, based on pairwise structure alignment with characterized enzymes from the same family. The native modules that were removed for recombinant protein expression in *P. pastoris* are represented in grey dashed lines. Protein 3D models were predicted by Alphafold3[35]. Enzyme modules and structures are colored according to their CAZy family. At: *Aspergillus terreus* ; Tv: *Talaromyces versatilis*.

and no activity can be detected on debranched RG-I extracted from *Arabidopsis* seed mucilage. Interestingly, *Tv*GH79 is not active on pNP-β-glucuronide but it is strongly active on gum Arabic, which is composed of type II arabinogalactans. Although several enzymes exhibit low activity on soybean RG-I, *Tv*GH53 is the only enzyme able to hydrolyze both soybean RG-I and SBM.

Semi-miniaturized hydrolysis of soybean meal

Since most of the produced enzymes cannot hydrolyze SBM pectin when used alone, we designed 12 enzymatic pools to identify suitable enzyme combinations leading to optimal degradation. Our objective was to evaluate in parallel all enzyme pools in triplicate, with and without the Rovabio™ cocktail, allowing us to screen a high number of potential combinations. To accommodate this, we developed a semi-miniaturized method using

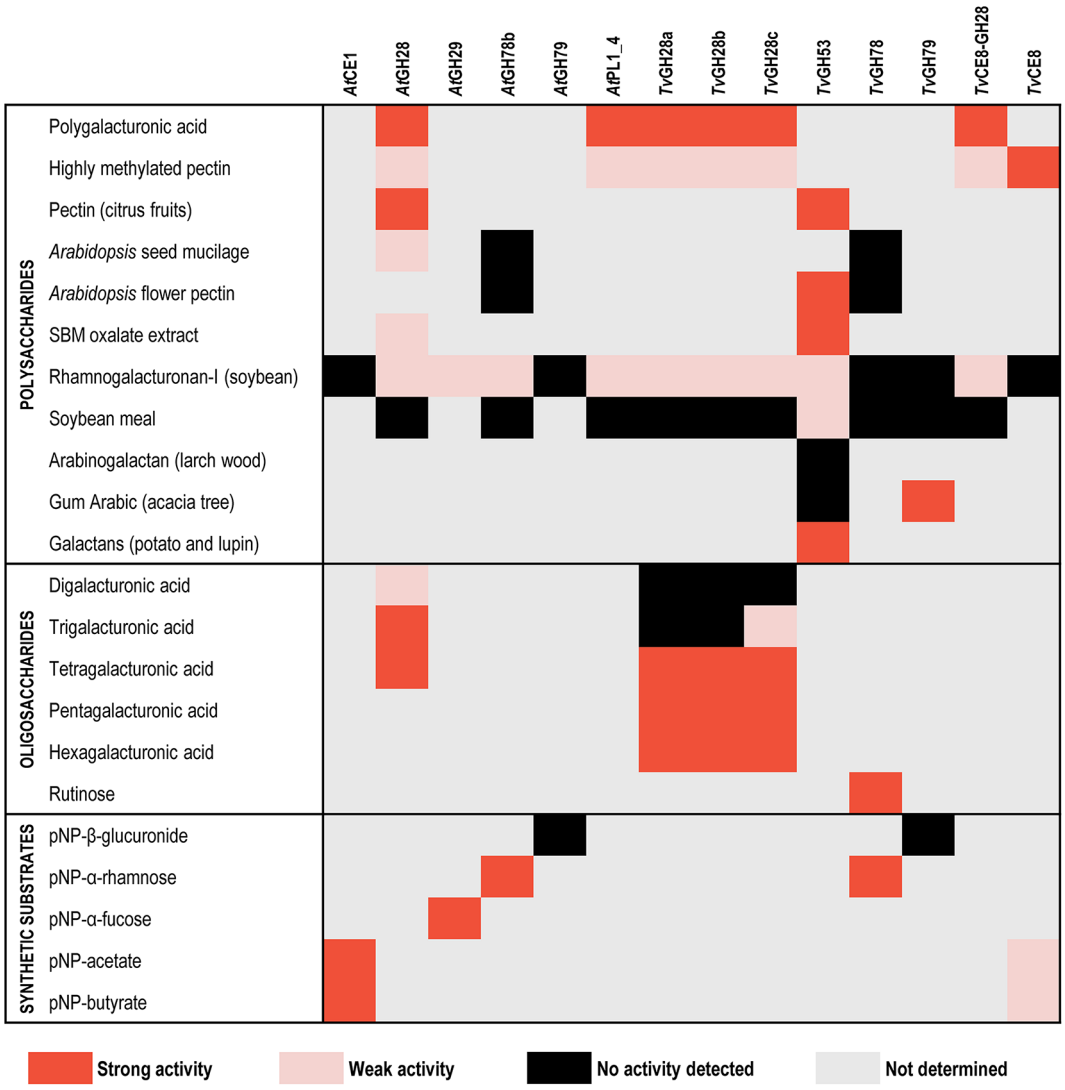

Fig. 2. Heatmap representation of the pectinolytic activities of the recombinant CAZymes on a library of 36 substrates. Activity was determined with purified enzymes. Experimental conditions and detection methods for enzymatic activity were adapted according to the substrate and the enzyme, as described in the methods section. *Tv*GH93 was tested on soybean meal, soybean RG-I, branched and debranched arabinans (sugar beet pulp), α-(1,5)-arabino-oligosaccharides (DP2 to DP6), arabinogalactan (larch wood), arabinoxylan (wheat), xylan (beechwood), xyloglucan (tamarind seed), lichenan (Icelandic moss), glucuronoarabinoxylan (wheat bran) and pNP-α-arabinofuranose but no activity was detected under the conditions assayed. Red corresponds to strong activity, pink to weak activity, black to no activity detected, and grey to undetermined activity. Under similar assay conditions, we defined a strong activity as the enzyme's primary activity, while a weak activity was considered a secondary activity.

96-deepwell plates, as shown in Fig. 3. Protocol optimizations identified a plate effect, meaning that analyzing the same sample on two different plates produced slightly different results. Since the primary goal was to compare the enzyme mixes to one another, rather than comparing enzyme mixes alone to mixes with Rovabio™ Advance, reactions with and without Rovabio™ were performed on separate plates. To address the plate effect, each plate included its own controls (i.e., control SBM without enzyme and control SBM with Rovabio™ Advance alone). This approach ensured that comparisons could be made between the samples and their respective controls within the same plate.

To assess the efficiency of the 12 enzymatic pools, we considered six markers: the percentage of SBM solubilization post-hydrolysis, and the quantification of reducing sugars, uronic acids, rhamnose, arabinose + galactose, and fucose in the soluble fraction to monitor pectin deconstruction. SBM solubilization was assessed by measuring the residual dry matter (RDM) remaining after enzyme hydrolysis, while the soluble sugars in the hydrolysis supernatants were quantified using spectrophotometric methods. To be as unbiased as possible, the pools were designed based on several criteria, such as the fungal origin of the enzymes (e.g., pools #3 and #4) or their putative targets. For example, pool #5 contains enzymes that target the pectin backbone,

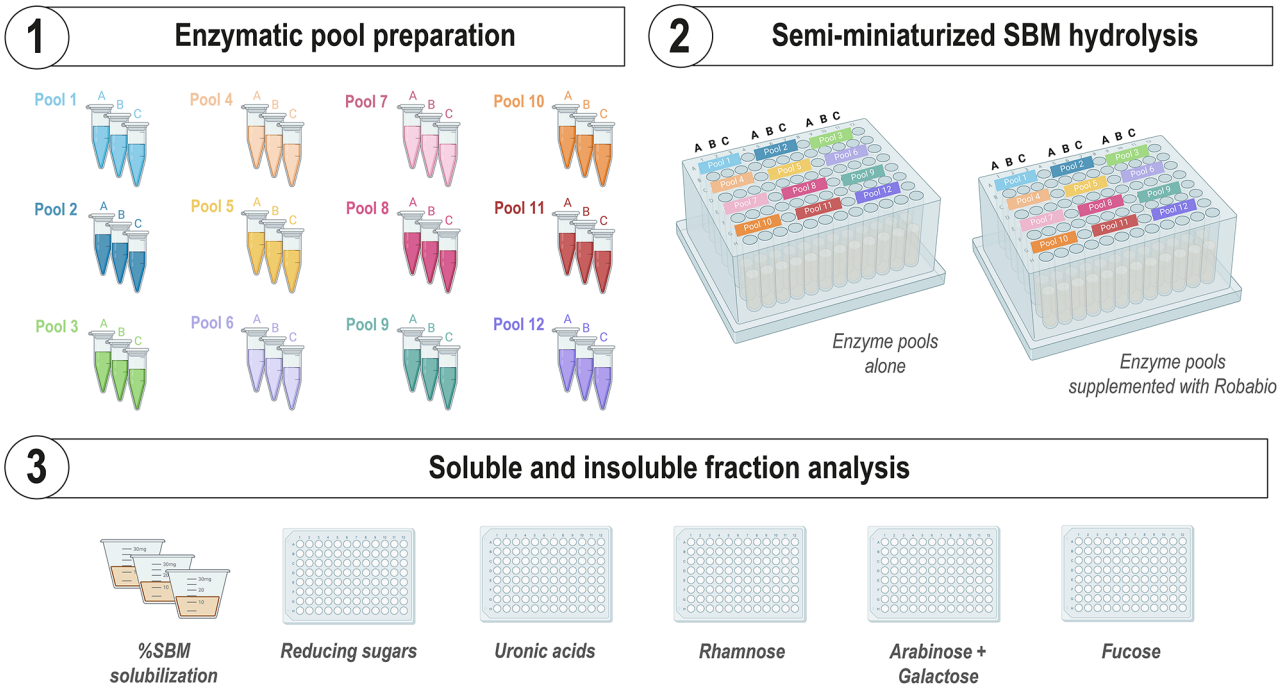

Fig. 3. Experimental set up for semi-miniaturized SBM hydrolysis by enzymatic pools. Each pool was prepared and tested in triplicate. Hydrolysis assays were performed at 37°C for 48 h. Quantification of reducing sugars was carried out using the DNS assay. Uronic acids, rhamnose, arabinose, galactose and fucose quantifications were performed using enzymatic commercial kits, as described in the material and Methods section. This figure was designed using BioRender software app.biorender.com.

while pool #6 contains enzymes targeting pectin side chains. While most pools were designed to be equimolar, pools #2 and #8 were adjusted according to the abundance of enzymes found in fungal secretomes by proteomic analysis in order to mimic *in vivo* conditions. The detailed composition of the pools is provided in Supplementary Table S2.

The strategy of designing multiple enzymatic pools based on different parameters proved effective, as shown by results observed across the different markers (Fig. 4). As expected, pools containing GH28 polygalacturonases released more uronic acids from SBM compared to pools #3, #6, #9, and #11, which lack enzymes targeting the pectin backbone. When comparing solubilization percentages (Fig. 4a) with sugar concentrations in the soluble fraction (Fig. 4c, e, g, and i), it appears that the key enzymes to increase SBM solubilization are targeting arabinose and galactose, found in pectin side chains.

Interestingly, all enzyme pools significantly enhanced the release of arabinose and galactose from SBM by Rovabio™ (p-value < 0.001; Fig. 4j), even those lacking enzymes specifically targeting pectin side chains. This suggests that the enzymes in the pools somehow improve access to arabinose- and galactose-containing saccharides for the Rovabio™ enzymes. Furthermore, 10 out of the 12 enzyme pools significantly enhance the release of uronic acids from SBM by Rovabio™ (p-value < 0.05), indicating a synergistic effect between the commercial cocktail and the selected enzymes for the pectin backbone hydrolysis. Although pool #4 is not the most efficient when used alone, it is the only one that significantly enhances Rovabio™ across all tested hydrolysis markers (p-value < 0.05). This pool is exclusively composed of *T. versatilis* enzymes (*Tv*GH28a, b and c, *Tv*GH53, *Tv*GH78, *Tv*GH79, *Tv*GH93, *Tv*CE8-GH28 and *Tv*CE8).

Identification of key pectinolytic enzymes involved in soybean meal degradation using a matrix-driven approach

To highlight the key enzymes involved in enhanced SBM pectin degradation, we conducted a Pearson correlation matrix with the hydrolysis data and the enzyme composition of the pools (Fig. 5). Interestingly, except for *At*PL1_4, all correlated enzymes originate from *T. versatilis* and can be found in pool #4. *Tv*GH53 shows a strong positive correlation with the release of arabinose and galactose from SBM, as well as with solubilization and the release of reducing sugars (p-value < 0.001). A similar trend is observed with *Tv*GH79, which is also involved in rhamnose hydrolysis when used alongside Rovabio™ (p-value < 0.01). Interestingly, while *Tv*GH93 displayed no detectable activity when tested alone, its presence in the enzyme pools correlates with the release of reducing sugars, arabinose, and galactose (p-value < 0.001). More surprisingly, *Tv*GH93 also contributes to rhamnose release when combined with Rovabio™ (p-value < 0.001). Out of the two GH78 rhamnosidases produced, only *Tv*GH78 correlates with the release of uronic acids from SBM (p-value < 0.001). It should also be noted that some enzymes are negatively correlated with hydrolysis markers, such as *At*CE1 and *At*GH79, which most likely hamper SBM solubilization and reducing sugars release when added to Rovabio™ (p-value < 0.01).

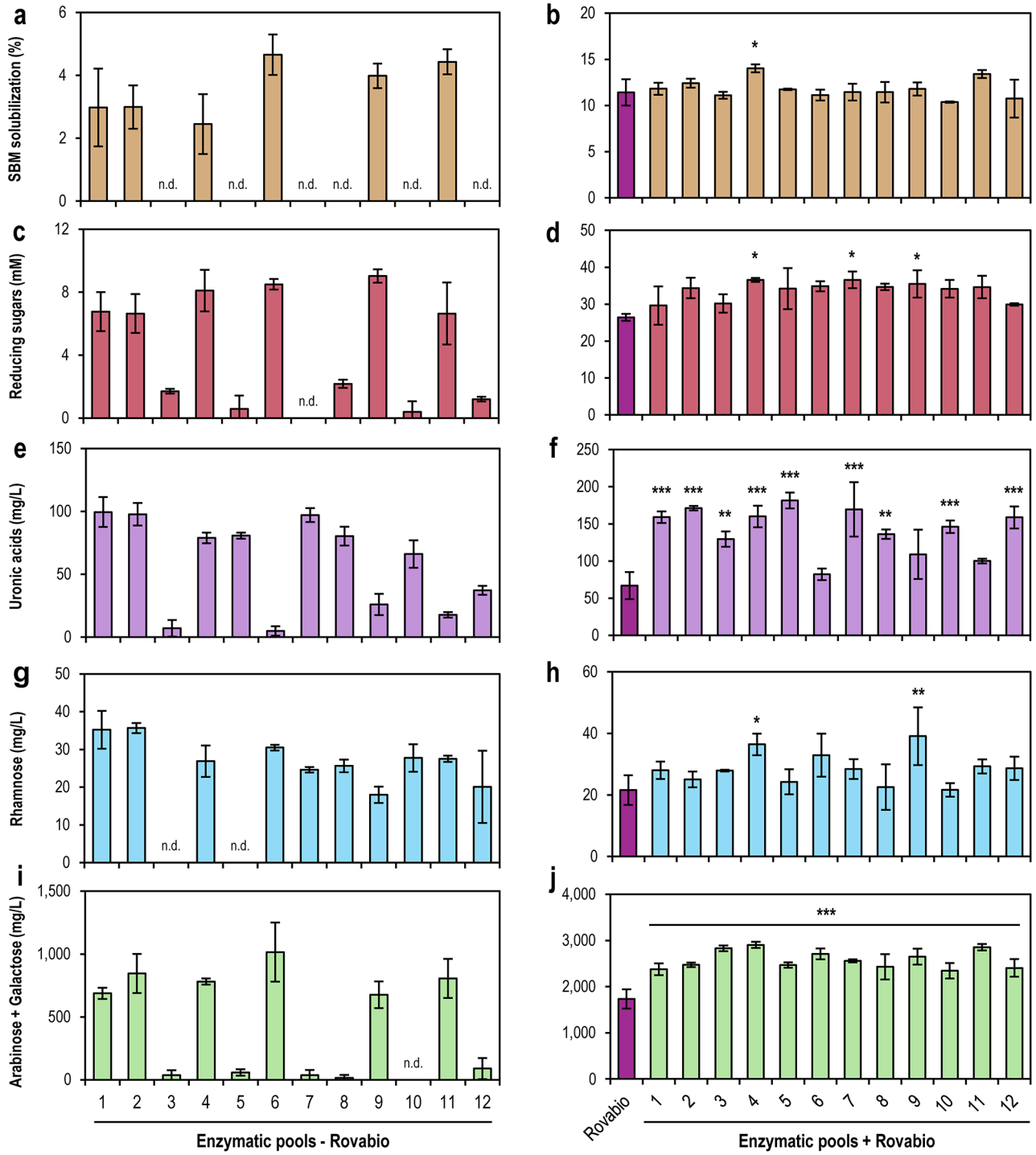

Fig. 4. Soybean meal hydrolysis by the 12 enzymatic pools with and without Rovabio™. (**a**,**b**) Percentage of SBM solubilization after hydrolysis by enzymatic pools (a) and by enzymatic pools + Rovabio™ (b). (**c**, **d**) Reducing sugars present in the soluble fraction after hydrolysis by enzymatic pools (c) and by enzymatic pools + Rovabio™ (d). (**e**, **f**) Total uronic acids in the soluble fraction after hydrolysis by enzymatic pools (e) and by enzymatic pools + Rovabio™ (f). (**g**, **h**) Rhamnose present in the soluble fraction after hydrolysis by enzymatic pools (g) and by enzymatic pools + Rovabio™ (h). (**i**,**j**) Arabinose + galactose released in the soluble fraction after hydrolysis by enzymatic pools (i) and by enzymatic pools + Rovabio™ (j). No fucose could be detected. Error bars correspond to standard deviations calculated from biological replicates ($n = 3$). Statistical analyses were performed using analysis of variance and post hoc Tukey's test, using Rovabio™ as reference sample. $^{*}P < 0.05$, $^{**}P < 0.01$, $^{***}P < 0.001$, n.d.: not detected.

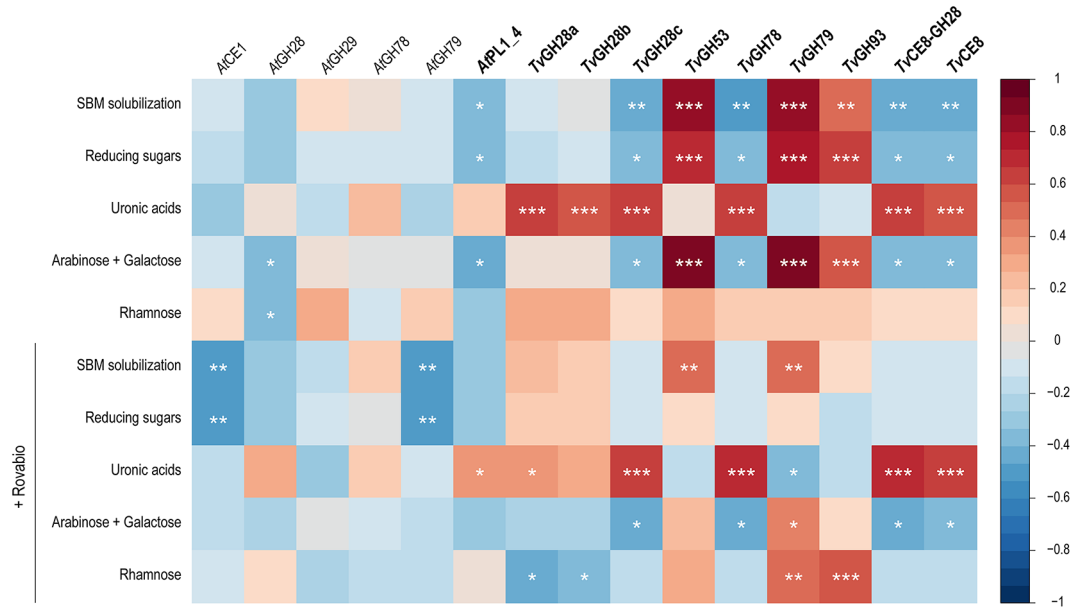

Fig. 5. Pearson correlation matrix highlighting the fungal CAZymes involved in soybean meal pectin degradation. The correlation matrix was constructed using the enzymatic composition of the pools (based on molarity) and the impact of each pool on selected hydrolysis markers. In total, the matrix includes 36 enzymatic pools (12 pools in biological triplicates), 15 enzymes, and 10 hydrolysis markers. Color code for Pearson correlation coefficient is indicated on the right. $^{*}P<0.05$, $^{**}P<0.01$, $^{***}P<0.001$.

To better understand the role of each correlated enzyme in SBM deconstruction, we assessed their specific activities on several substrates (Supplementary Figures S2–S7). *Tv*GH28a, b, and c function as exo-acting polygalacturonases with a strong preference for polygalacturonic acid over methylated pectin and soybean RG-I (Supplementary Figure S2). A similar preference is observed for *At*PL1_4 and *Tv*CE8-GH28 (Supplementary Figure S3). Moreover, pre-treating methylated pectin with *Tv*CE8 increased the release of Gal*A* by GH28 enzymes by up to 9-fold compared to untreated methylated pectin (Supplementary Figure S4). *Tv*GH53 exhibits high specificity for potato and lupin galactans, producing galacto-oligosaccharides of varying polymerization degrees, which confirms its endo-β-(1,4)-galactanase activity (Supplementary Figure S5). *Tv*GH78 shows higher specific activity on pNP-α-rhamnose than on rutinose, confirming its α-rhamnosidase activity while indicating that α-(1,6)-rhamnose is not its favored target (Supplementary Figure S6). Finally, the activity of *Tv*GH79 on gum Arabic reveals that it displays a rhamnosyl-β-glucuronidase activity, being capable of hydrolyzing a Rha-Glc*A* disaccharide from the side chains of type II AG (Supplementary Figure S7).

According to the enzymes' specific activities and the GC-MS linkage analysis performed on the oxalate extract of SBM (Supplementary Figure S8), we propose a structural model for soybean meal pectin (Fig. 6). The identification of *Tv*GH79 through the Pearson correlation matrix indicates the presence of the Rha-Glc*A* disaccharide in the AG side chains of soybean pectin. In a similar way, the correlation between *Tv*CE8 and uronic acid release from SBM (p-value < 0.001) suggests the presence of methyl-ester on the backbone of soybean pectin. The positive correlation of *Tv*GH93 with the release of both arabinose and rhamnose allows to formulate several hypotheses. Since *Tv*GH93 is not active on debranched α-(1,5)-arabinans nor on α-(1,5)-arabinans branched with α-(1,3)-arabinose, we suggest that it could either target *(i)* the L-Rha-α-(1,4)-L-Ara linkage between the RG-I backbone and its side chains, *(ii)* the single α-(1,2)-arabinose substitution on the arabinan chain or *(iii)* the double α-(1,2)/α-(1,3)-arabinose substitution on the arabinan chain (Fig. 6).

Discussion

In this study, we successfully identified several key fungal enzymes involved in SBM pectin degradation using a multi-enzyme approach. As previously shown for lignocellulosic and hemicellulose-rich substrates[36], the deconstruction of soybean pectin is not a one-enzyme job. Indeed, most of the CAZymes we investigated are not active on SBM when used alone. This observation echoes with the human gut bacteria pectinolytic system that requires up to 20 different enzymes, often organized as Polysaccharide Utilization Loci (PULs)[11,17]. As fungi do not possess PULs, the identification of fungal enzymes active on a specific substrate needs to be investigated by comparative secretomic analysis, which can be fine-tuned with correlation matrixes[33,37,38].

In line with the minimal cocktail approach used by Meyer and colleagues[36], we observed that the enzymatic pools containing all recombinant enzymes (i.e., pools #1 and #2) are not necessarily the most efficient ones. This indicates that some antagonism might arise when enzymes are blended together, rather than being combined in a more strategic manner. Some of the enzymes we selected might be highly specific or preferentially target decorated substrates. We can hypothesize that the removal of some substitutions could either modify pectin solubility or its interactions with other plant polysaccharides, hampering enzyme accessibility[39,40]. This could

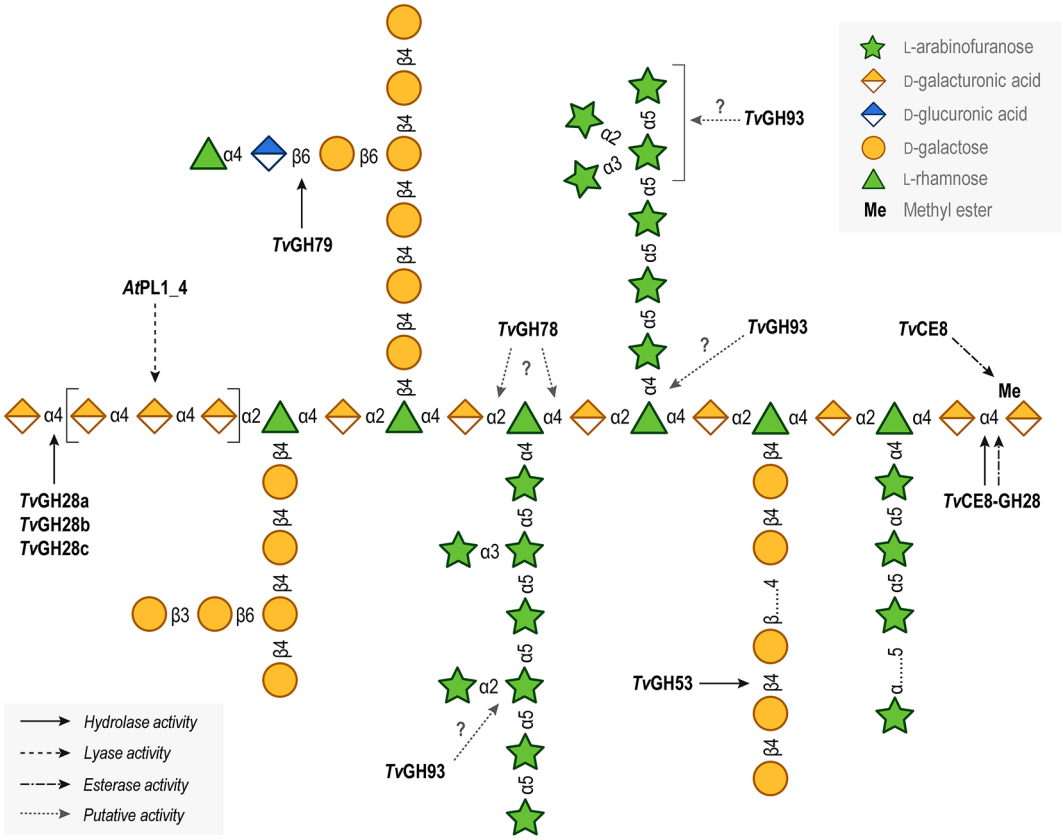

Fig. 6. Proposed structural model for soybean meal pectin. This model was established according to the activity of the enzymes highlighted by the Pearson matrix and the linkage analysis of soybean meal pectin by GC-MS. The model does not account for residues and linkages abundances, which are displayed in Supplementary Figure S8.

explain why some enzymes show a negative correlation with hydrolysis markers when added to Rovabio™. Our findings highlight the importance of a more rational approach for the design of tailored enzymatic cocktails, instead of relying on universal solutions. For instance, this issue was tackled in the bioethanol production industry through computer-assisted design of enzymatic cocktails[41].

Although the Pearson correlation matrix highlights *Tv*GH93 as a key enzyme for SBM hydrolysis, its activity was not detected using arabinose-containing oligo- or polysaccharides. This absence of activity could be due to substrate inaccessibility. Previously characterized enzymes from GH93 family possess exo-α-(1,5)-arabinanase activity[42,43], however several substitutions have been reported in the side chains of RG-I[9,11,16]. These decorations could be essential for substrate recognition by *Tv*GH93, as it was previously reported for arabinofuranosidases active on arabinoxylan[44–46]. To support this hypothesis, multiple sequence alignment revealed that *Tv*GH93 shares less than 25% sequence identity with characterized enzymes from the same CAZy family. Additionally, pairwise structural alignment with Arb93A from *Fusarium oxysporum*, which is the closest characterized GH93 family member to *Tv*GH93, reveals significant structural differences between the two enzymes. Indeed, *Tv*GH93 features a more open and negatively charged active pocket compared to Arb93A. Moreover, several residues at the −2 subsite of Arb93A are different in *Tv*GH93 (Supplementary Figure S9)[47]. These findings strongly suggest a distinct substrate specificity for *Tv*GH93, which remains to be unveiled.

Interestingly, *Tv*GH53 is the only enzyme identified by the Pearson correlation matrix that is active on both soybean meal and soybean RG-I when used alone. It displays higher activity on β-(1,4)-galactans from potato and lupin, but no activity can be determined on β-(1,3) nor on mixed β-(1,3)/β-(1,6)-arabinogalactans (AG) from larch wood and gum Arabic. Many studies have reported the presence of AG of types I and II in the side chains of RG-I[48–53], and both RG-I and AG proteins have been found to be covalently linked in the cell wall of *Arabidopsis*[16]. Therefore, the lower specific activity of *Tv*GH53 on soybean RG-I compared to potato galactans could be explained by its sensitivity to the β-(1,3)/β-(1,6)-galactose decorations in the side chains of soybean RG-I.

Other interesting features of SBM pectin structure were revealed by our approach. For instance, although *Tv*CE8 alone showed no detectable activity on SBM, its correlation with the release of uronic acids from SBM suggests that the pectin backbone is methylesterified. This finding is quite surprising, given the intense processing that soybeans undergo during oil extraction[54], where alkaline conditions would typically be expected to cause de-esterification of polysaccharides. On another note, we found that *Tv*GH79 is highly specific for gum Arabic, indicating it is a rhamnosyl-glucuronidase as recently described in *Fusarium oxysporum*[55]. *Tv*GH79

is the second fungal enzyme from the GH79 family to be reported with this specific activity. It indicates the presence of AG-II in SBM.

Out of the 15 fungal CAZymes studied herein, we showed that the enzymes originating from *T. versatilis* are the best to supplement Rovabio™ for SBM pectin degradation. Considering the commercial enzymatic cocktail is also produced by *T. versatilis*[24,56], this observation supports previous works highlighting the strong enzymatic potential of this fungus for complex polysaccharide degradation in a biotechnological context[57–62].

Conclusions

Our work presents an innovative approach to decipher pectin complexity in biotechnologically relevant substrates, like soybean meal. By designing multi-activity enzymatic cocktails in combination with a correlation matrix, we demonstrated that adopting a broader perspective can often lead to more nuanced discoveries. Analyzing the enzymes as pools enabled the identification of key enzymes that might have been overlooked if studied individually. We expect this research will enhance the valorization of soybean meal and other agricultural co-products by pinpointing essential activities for their degradation, ultimately maximizing nutrient-rich substrates and reducing industrial waste.

Methods

Materials

Unless stated otherwise, chemicals and reagents were purchased from SigmaAldrich® (Burlington, MA, USA). Soybean RG-I, potato and lupin galactans, larch arabinogalactans, branched and debranched arabinans, xylan, xyloglucan, lichenan, arabinoxylan and oligogalacturonides (DP2 to DP4) were purchased from Megazyme® (Bray, Ireland). Highly methylated pectin, rutinose and pNP-α-rhamnose were purchased from Biosynth® (Staad, Switzerland). pNP-β-glucuronide was purchased from Santa Cruz Biotechnology® (Dallas, Texas, USA). Oligogalacturonides of DP5 and DP6 were purchased from Elicityl® (Crolles, France). The soybean meal (SBM) mixture was supplied by Adisseo® France SAS. It consists of an equal dry weight ratio of five SBM batches from various origins: two from SojaProtein (SOPRO UTG and GRIT48, Serbia), one from Terrena (France), one from BRF-NovaMutum (Brazil - Midwest), and one from India, all ground to a thickness of 3 mm. Nonadherent mucilage from *Arabidopsis thaliana* ecotype Columbia-0 (Col-0) seeds was prepared and analyzed following previously published protocols[63]. Specifically, *Arabidopsis thaliana* Col-0 seeds were hydrated in deionized water for 10 min, then sonicated with a probe sonicator (Qsonica) for 1 min. The material was filtered through a 50 µm nylon mesh, dialyzed against deionized water for 2 days using 3.5 K MWCO dialysis tubing (Ward's Science), and subsequently freeze-dried using a lyophilizer (VirTis). *Arabidopsis* (Col-0) seeds were grown on a 1:1 soil mix of Metromix 830 (Sungro, USA) and vermiculite, supplemented with Plant Food (Sta-Green, USA) and Osmocote Smart-Release Plant Food Flower & Vegetable (Scotts, USA). Seeds were stratified for 2 days at 4 °C before being transferred to a Conviron growth chamber (Canada) set to an 18 h light/6 h dark cycle at 21 °C with a light intensity of 120 µmol photons $m^{-2}.s^{-1}$. Flowers were harvested from 6-week-old plants, homogenized in 80% ethanol using a Polytron® Homogenizer (Brinkmann Instrument), and filtered through a 50 µm nylon mesh. The residue was washed with 80% ethanol and stirred overnight in a 1:1 chloroform/methanol solution. It was then filtered, washed with chloroform/methanol, followed by acetone, and left to dry in a fume hood. The resulting alcohol-insoluble residues (AIR) were suspended in 0.1 M sodium acetate (pH 5) and treated with Spirizyme Excel and Liquozyme SC DS (Novozymes) at 50 °C for 24 h to remove starch and cellulose. The de-starched AIR was filtered, washed with 0.1 M sodium acetate (pH 5), and resuspended in 0.5% ammonium oxalate (pH 5). After a day of incubation at room temperature with agitation, the suspension was centrifuged at 2683 *g* for 10 min. The supernatant was filtered through a GF/B glass microfiber filter (Whatman), dialyzed against deionized water for 2 days using 3.5 K MWCO dialysis tubing (Ward's Science), and freeze-dried on a lyophilizer (VirTis). Rovabio™ Advance was provided by Adisseo® France SAS. The same batch of the liquid concentrated form, stabilized with 0.35% (w/w) of sodium benzoate, was used for all hydrolysis tests.

Cloning and expression of recombinant enzymes

The proteins were produced using the in-house 3PE platform (*Pichia pastoris* protein express ; www.platform3pe.com). The nucleotide sequences coding for *At*CE1 (UniProt ID Q0CB21), *At*GH28 (UniProt ID Q0CXI3), *At*GH29 (UniProt ID Q0CDX3), *At*GH78b (UniProt ID Q0CTR2), *At*GH79 (UniProt ID Q0CNM8), *At*PL1_4 (UniProt ID Q0CFE1) from *Aspergillus terreus* and *Tv*GH28a (GenBank ID PQ761551), *Tv*GH28b (GenBank ID PQ761552), *Tv*GH28c (C-terminal domain of GenBank ID PQ761557), *Tv*GH53 (GenBank ID PQ761553), *Tv*GH78 (GenBank ID PQ761554), *Tv*GH79 (GenBank ID PQ761555), *Tv*GH93 (GenBank ID PQ761556), *Tv*CE8-GH28 (GenBank ID PQ761557) and *Tv*CE8 (N-terminal domain of GenBank ID PQ761557) from *Talaromyces versatilis* were synthesized after codon optimization for expression in *P. pastoris* (syn. *Komagataella phaffii*). Each gene was inserted into the expression vector pPICZαA (Invitrogen®, Carlsbad, California, USA) using *XhoI* and *XbaI* restriction sites in frame with the α-secretion factor at the N-terminus (i.e., without native signal peptide) and with a $(His)_6$tag at the C-terminus (without *c*-myc epitope) (Genewiz®, Leipzig, Germany). Transformation of competent *P. pastoris* X33 and selection of zeocin-resistant *P. pastoris* transformants screened for protein production were carried out as previously described[64]. The best-producing transformants were conserved as glycerol stock at -80 °C.

Heterologous protein production in flasks

All proteins were produced in 2-liter Erlenmeyer flasks. To this end, single colonies of *P. pastoris* X33 expressing each gene of interest were individually streaked on a YPD (yeast extract, peptone, and dextrose) agar plate and incubated for 3 days at 30 °C. A single colony was then used to inoculate 5 mL of YPD, in a 50-mL sterile

Falcon tube, and incubated for 5 h (30 °C, 160 *rpm*). This preculture was used to inoculate at 0.2% (v/v) 500 mL of BMGY (buffered glycerol complex medium), in a 2-liter Erlenmeyer flask, and incubated for approximately 16 h (30 °C, 200 *rpm*) until OD_{600} (optical density at 600 nm) reached 4 to 6. The produced cellular biomass was harvested by centrifugation (5 min, 15 °C, 4000 *g*) and the cell pellet was then resuspended in 100 mL of BMMY (buffered methanol complex medium) supplemented with methanol (3%, v/v). The culture was incubated for 3 days (20 °C, 200 *rpm*), with daily additions of methanol (3% added, v/v). Then, the extracellular medium was recovered by centrifugation (10 min, 4 °C, 4000 *g*), and the supernatant was filtered on 0.45 µm membrane (Millipore®, Massachusetts, USA) and stored at 4 °C before purification.

Protein purification

Filtered and pH-adjusted culture supernatants were loaded onto a 5 mL HisTrap™ Excel column (Cytiva®, Illkirch, France) pre-equilibrated with buffer A (Tris-HCl 50 mM pH 7.8, NaCl 150 mM, imidazole 10 mM) that was connected to an Äkta purifier 100 (Cytiva®). Elution of $(His)_6$tagged recombinant proteins was done with a gradient of buffer B (Tris-HCl 50 mM pH 7.8, NaCl 150 mM, imidazole 500 mM). Protein fractions were loaded on 4–20% Stain free Tris-Glycine precast SDS-PAGE gels (Bio-Rad, Hercules, USA), and fractions containing the recombinant proteins were pooled. Buffer exchange was performed to remove imidazole by loading the samples onto a HiPrep™ 26/10 Desalting column (Cytiva®) against Tris-HCl 50 mM pH 7.8, NaCl 150 mM buffer. Proteins were then concentrated on Vivaspin® 20 (10 kDa cut-off, polyethersulfone ; Sartorius, Göttingen, Germany) and their final concentration was determined by absorption at 280 nm using a Nanodrop ND-2000 spectrophotometer (Thermo Fisher Scientific®, Waltham, MA, USA) and the extinction coefficients listed in Supplementary Table S1.

Enzymatic hydrolysis of soybean meal

Hydrolysis tests were conducted as previously described[33]. The reactions took place in 2 mL of sodium acetate buffer (50 mM, pH 5.2) at 37°C for 48 h. These were performed in 96-deepwell 2 mL round-bottom plates containing 150 mg of SBM. The plates were thermally sealed with aluminum foil to prevent evaporation and incubated in an Infors Multitron® plate shaker at 850 *rpm* with 3 mm orbital shaking. Rovabio™ Advance was added at a concentration of 0.9 mg of total proteins per reaction. Enzymatic pools were prepared in triplicates and the volumes added in the reactions were calculated according to the enzyme concentrations presented in Supplementary Table S2. After hydrolysis, SBM insoluble fractions were separated from the soluble fractions by centrifugation in swing buckets at maximal speed for 20 min at 4 °C. Then, SBM pellets were washed twice in distilled water and the residual dry matter (RDM) was weighed after heating at 105 °C for 48 h. The percentage of SBM residual dry matter was calculated with Eq. (1).

$$Residual\ dry\ matter\ (RDM, \%) = \frac{Mass\ of\ dry\ matter\ after\ hydrolysis\ \ (mg)}{Mass\ of\ dry\ matter\ before\ hydrolysis\ \ (mg)} \quad (1)$$

The percentage of solubilization was then calculated by comparing the residual dry matter of the enzyme-treated samples to that of the SBM control without enzyme, which underwent the same treatment conditions, according to Eq. (2).

$$SBM\ solubilization\ (\%) = \%\ RDM_{no\ enzyme}\ -\ \%\ RDM_{enzyme} \quad (2)$$

To stop the enzymatic reaction, the soluble fractions of SBM were diluted 1:1 with 0.2 M NaOH and filtered through 0.45 µm 96-well filtration plates (AcroPrep Advance, 1 ml, 0.45 µm, Supor Natural PP, Pall Corporation®, New York, USA). The soluble fractions were stored at +4 °C for up to 5 days or at -20 °C for longer periods to prevent sample degradation. Reducing sugars concentration in these fractions were determined using the 3,5-dinitrosalicylic acid (DNS) assay[65], as previously described[66]. Quantification was based on a standard range of D-glucose, ranging from 0.125 to 10 mM. Pectin sugar monomers in these fractions were quantified using enzymatic assay kits from Megazyme®. The kits K-uronic, K-rhamnose, K-arga, and K-fucose were used to detect D-glucuronic/ D-galacturonic acids, L-rhamnose, L-arabinose/D-galactose, and L-fucose, respectively. The assays were conducted in UV Star microplates (Thermo Fischer Scientific®) following the supplier's instructions. Quantifications were based on the supplied standards, ranging from 0.3 to 15 µg for uronic acids and rhamnose, 0.2–12 µg for arabinose and galactose, and 0.3–7.5 µg for fucose.

Enzymatic activity assays

Screening for enzyme activity on soybean RG-I was done at 37°C and 1000 *rpm* in sodium acetate buffer (50 mM, pH 5.2) with 2.5% (w/v) substrate and 5 µg/mL of enzyme. Activity was determined by quantification of reducing sugars with the DNS assay after 24 h of hydrolysis[66]. *At*CE1 activity on pNP-acetate and pNP-butyrate was determined at 37°C and 800 *rpm* for 30 min using 1.5 µM of enzyme and 1 mM of substrate as previously described[38]. *At*GH29 activity assays on pNP-α-fucose were done similarly, with 3 µM enzyme. Alpha-rhamnosidase activity determination on pNP-α-rhamnose was carried out with 0.5 mM substrate and 50 nM *At*GH78b or *Tv*GH78. Beta-glucuronidase activity determination on pNP-β-glucuronide was carried out with 1 mM substrate and 100 nM *At*GH79 or *Tv*GH79. Enzymes specific activity determinations were done in triplicate in sodium acetate buffer (50 mM, pH 5.2) at 40°C and 1000 *rpm*. Time reactions were adapted according to enzyme's initial velocity. Released products were analyzed by HPAEC-PAD. Rutinose was used at 1 mM with 10 nM of *Tv*GH78 enzyme. Oligogalacturonides (DP2 to DP6) were used at 0.4 mM with 2.5–10 nM of GH28 enzymes. Arabino-oligosaccharides (DP2 to DP6) were used at 0.4 mM with 100 nM of *Tv*GH93. Soybean meal was used at 1% (w/v) with 10 nM of *Tv*GH28a, b or c, 25 nM of *Tv*GH53, 50 nM of *Tv*GH78, 100

nM of *At*GH78b, *At*PL1_4, *Tv*CE8-GH28, *Tv*GH79 or *Tv*GH93. Potato and lupin galactans were used at 1% (w/v) with 5 nM of *Tv*GH53. Xylan, arabinoxylan, xyloglucan, lichenan, branched and debranched arabinans were used at 1% (w/v) with 100 nM of *Tv*GH93. Larch arabinogalactan was used at 1% (w/v) with 25 nM of *Tv*GH53 or 100 nM of *Tv*GH93. SBM oxalate extract, *Arabidopsis* flower pectin and seed mucilage were used at 0.1% (w/v) with 10–20 nM of *Tv*GH53, 10 nM of *At*GH78b or *Tv*GH78. Gum Arabic was used at 0.5% (w/v) and 10 nM of *Tv*GH53 or 5 nM of *Tv*GH79. Highly methylated pectin (HMP) was used at 1% (w/v) with 5 nM of *Tv*GH28a, 10 nM of *Tv*GH28b or *Tv*GH28c, 50 nM of *Tv*CE8-GH28 or *At*PL1_4. Polygalacturonic acid was used at 1% (w/v) with 2 nM of *Tv*GH28a or *Tv*GH28b, 10 nM of *Tv*GH28c, 50 nM of *Tv*CE8-GH28 or *At*PL1_4. Enzymatic interplays between *Tv*CE8 and GH28 enzymes were done in triplicates by pretreating 1% (w/v) of HMP with 0.1 µM of *Tv*CE8 for 1 h at 40 °C and 1000 *rpm* in sodium acetate buffer (50 mM, pH 5.2). *Tv*CE8 was then inactivated by boiling for 5 min and 0.5% of the resulting pretreated HMP was incubated with 50 nM of GH28 enzymes for 20 min. The same procedure was done without *Tv*CE8 as a control. Released Gal*A* was then quantified by HPAEC-PAD, as described below.

HPAEC-PAD analyses

The detection method is performed using a high-performance anion-exchange chromatography (HPAEC) coupled with pulsed amperometric detection (PAD) (DIONEX ICS6000 system, Thermo Fisher Scientific®), as previously described[33]. The system is equipped with a CarboPac-PA1 guard column (2 × 50 mm) and a CarboPac-PA1 column (2 × 250 mm) kept at 30°C. Elution was carried out at a flow rate of 0.25 mL/min and 25 µL of samples was injected. The eluents used were 100 mM NaOH (eluent A) and NaOAc (1 M) in 100 mM NaOH (eluent B). The initial conditions were set to 100% eluent A, and the following gradient was applied: 0 to 10 min, 0 to 10% B; 10 to 35 min, 10 to 35% B (linear gradient); 35 to 40 min, 30 to 100% B (curve 6); 40 to 41 min, 100 to 0% B; 41 to 50 min, 100% A. Integration was performed using the Chromeleon 7.2.10 data software (Thermo Scientific®).

LC-MS analyses for rhamnosyl-α-(1,4)-glucuronate detection

Samples were filtered (0.2 µm, Chromafil®, Macherey-Nagel, France) and diluted 2-fold with Acetonitrile 100%. The presence of rhamnosyl-α-(1,4)-glucuronate was confirmed by Ultra High Performance Liquid Chromatography (UHPLC, UltiMate™ 3000 Rapid Separation (RS) HPLC Systems, Thermo Scientific®) coupled to charged aerosol detector (CAD), and an ISQ-EM mass spectrometer (Thermo Scientific®). HILIC separation was performed on an Amide column (Waters, 1.7 µm, 150 × 2.1 mm) at a flow rate of 0.4 mL/min at 35 °C and using isocratic condition. The mobile phase was 20% solvent A (Ammonium formate 15 mM) and 80% solvent B (Acetonitrile 100%). Negative-ion ESIMS spectra (110–800 m/z) were acquired setting vaporizer temperature at 117 °C, ion transfer tube temperature at 300 °C, sheath gas pressure at 28.8 psig, auxiliary gas pressure at 3.2 psig, and sweep gas pressure at 0.5 psig. UHPLC-CAD-ESI-MS data were acquired and analyzed with Chromeleon v7.2.10 data software (Thermo Scientific®).

Extraction of soybean meal pectin fraction

The SBM oxalate extract was prepared as alcohol insoluble residue (AIR) and fractionated according to established methods with some modifications[67]. Briefly, SBM AIR was suspended in 0.5% ammonium oxalate (pH 5) and shaken at room temperature at 250 *rpm* overnight, then filtered through a 50 µm nylon mesh followed by a GF/A glass microfiber filter. The filtrate was dialyzed against deionized water using 3.5 K MWCO dialysis tubing for 2 days in a cold room, with intermittent changes of water. After dialysis, the filtrate was centrifuged, and the supernatant was lyophilized to obtain oxalate soluble pectins.

Linkage analysis by GC-MS

Glycosyl linkage analysis was performed by combined gas chromatography-mass spectrometry (GC-MS) of the partially methylated alditol acetates (PMAAs) derivatives produced from the samples. The procedure is a slight modification of the one described by Black and colleagues[63]. Briefly, the samples were acetylated using N-methylimidazole and acetic anhydride in the ionic liquid 1-ethyl-3-methylimidazolium acetate [Emim][Ac]. The acetylated samples were dialyzed against DI water for 3 days in a 3.5-kDa MWCO dialysis membrane. The samples were then methylated using dimsyl potassium base. Following DCM extraction, the carboxylic acid methyl esters were reduced using lithium aluminum deuteride (LiAlD4) in THF (80 °C, 4 h). After a second dialysis as before, the samples were remethylated using two rounds of treatment with sodium hydroxide (15 min each) and methyl iodide (45 min each). The samples were then hydrolyzed using 2 M TFA (2 h in sealed tube at 120 °C), reduced with NaBD4, and acetylated using acetic anhydride/TFA. The resulting PMAAs were analyzed on an Agilent 7890 A GC interfaced to a 5975 C MSD (mass selective detector, electron impact ionization mode). Separation was performed on a 30 m Supelco SP-2331 bonded phase fused silica capillary column.

Statistical tests

One-way analysis of variance and post hoc Tukey's honestly significant difference were performed on the hydrolysis data using an online calculator (statskingdom.com) with a significance level (α) of 0.05. The correlation matrix was established with a Pearson statistical test at 0.95 confidence level, using the RStudio software for Windows (version 2022.07.2; Posit Software, PBC, Boston, MA, USA). Calculation of the matrix was performed by the R Stats Package (version 4.2.2), while the visualization was done using the corrplot package (version 0.92). The matrix was performed using the molar concentrations of the enzymes in the enzymatic pools and the values obtained for each hydrolysis marker tested. Both the raw values and the improvement folds compared to Rovabio™ alone were injected in the matrix.

Data availability

Data are provided within the manuscript and supplementary information files.

Received: 23 October 2024; Accepted: 13 December 2024
Published online: 11 January 2025

References

1. Varner, J. E. & Lin, L. S. Plant cell wall architecture. *Cell* **56**, 231–239 (1989).
2. Höfte, H. & Voxeur, A. Plant cell walls. *Curr. Biol.* **27**, R865–R870 (2017).
3. Kaczmarska, A., Pieczywek, P. M., Cybulska, J. & Zdunek, A. Structure and functionality of Rhamnogalacturonan I in the cell wall and in solution: A review. *Carbohydr. Polym.* **278**, 118909 (2022).
4. Zdunek, A., Pieczywek, P. M. & Cybulska, J. The primary, secondary, and structures of higher levels of pectin polysaccharides. *Compr. Rev. Food Sci. Food Saf.* **20**, 1101–1117 (2021).
5. Ropartz, D. & Ralet, M. C. Pectin structure. In *Pectin: Technological and Physiological Properties* (ed Kontogiorgos, V.) 17–36 https://doi.org/10.1007/978-3-030-53421-9_2 (Springer International Publishing, 2020).
6. Levigne, S., Thomas, M., Ralet, M. C., Quemener, B. & Thibault, J. F. Determination of the degrees of methylation and acetylation of pectins using a C18 column and internal standards. *Food Hydrocoll.* **16**, 547–550 (2002).
7. Schols, H. A., Bakx, E. J., Schipper, D. & Voragen, A. G. J. A xylogalacturonan subunit present in the modified hairy regions of apple pectin. *Carbohydr. Res.* **279**, 265–279 (1995).
8. Mort, A., Zheng, Y., Qiu, F., Nimtz, M. & Bell-Eunice, G. Structure of xylogalacturonan fragments from watermelon cell-wall pectin. Endopolygalacturonase can accommodate a xylosyl residue on the galacturonic acid just following the hydrolysis site. *Carbohydr. Res.* **343**, 1212–1221 (2008).
9. Ha, M. A., Viëtor, R. J., Jardine, G. D., Apperley, D. C. & Jarvis, M. C. Conformation and mobility of the arabinan and galactan side-chains of pectin. *Phytochemistry* **66**, 1817–1824 (2005).
10. Huisman, M. M. H. et al. The occurrence of internal (1→5)-linked arabinofuranose and arabinopyranose residues in arabinogalactan side chains from soybean pectic substances. *Carbohydr. Res.* **330**, 103–114 (2001).
11. Luis, A. S. et al. Dietary pectic glycans are degraded by coordinated enzyme pathways in human colonic *Bacteroides*. *Nat. Microbiol.* **3**, 210–219 (2018).
12. Cipriani, T. R. et al. Gastroprotective effect of a type I arabinogalactan from soybean meal. *Food Chem.* **115**, 687–690 (2009).
13. Munarin, F., Tanzi, M. C. & Petrini, P. Advances in biomedical applications of pectin gels. *Int. J. Biol. Macromol.* **51**, 681–689 (2012).
14. Pellerin, P., Vidal, S., Williams, P. & Brillouet, J. M. Characterization of five type II arabinogalactan-protein fractions from red wine of increasing uronic acid content. *Carbohydr. Res.* **277**, 135–143 (1995).
15. Saulnier, L. & Thibault, J. F. Ferulic acid and diferulic acids as components of sugar-beet pectins and maize bran heteroxylans. *J. Sci. Food Agric.* **79**, 396–402 (1999).
16. Tan, L. et al. Most of the rhamnogalacturonan-I from cultured *Arabidopsis* cell walls is covalently linked to arabinogalactan-protein. *Carbohydr. Polym.* **120340** https://doi.org/10.1016/j.carbpol.2022.120340 (2022).
17. Ndeh, D. et al. Complex pectin metabolism by gut bacteria reveals novel catalytic functions. *Nature* **544**, 65–70 (2017).
18. Drula, E. et al. The carbohydrate-active enzyme database: functions and literature. *Nucleic Acids Res.* **50**, D571–D577 (2022).
19. Hage, H. & Rosso, M. N. Evolution of fungal carbohydrate-active enzyme portfolios and adaptation to plant cell-wall polymers. *J. Fungi.* **7**, 185 (2021).
20. Couturier, M. et al. Fungal secretomics of ascomycete fungi for biotechnological applications. *Mycosphere J.* **7**, 1546 (2016).
21. Ribeaucourt, D., Bissaro, B., Lambert, F., Lafond, M. & Berrin, J. G. Biocatalytic oxidation of fatty alcohols into aldehydes for the flavors and fragrances industry. *Biotechnol. Adv.* **107787** https://doi.org/10.1016/j.biotechadv.2021.107787 (2021).
22. Filiatrault-Chastel, C., Heiss-Blanquet, S., Margeot, A. & Berrin, J. G. From fungal secretomes to enzymes cocktails: The path forward to bioeconomy. *Biotechnol. Adv.* **52**, 107833 (2021).
23. Plouhinec, L., Neugnot, V., Lafond, M. & Berrin, J. G. Carbohydrate-active enzymes in animal feed. *Biotechnol. Adv.* **65**, 108145 (2023).
24. Bampidis, V. et al. Safety and efficacy of a feed additive consisting of endo-1,4-beta-xylanase and endo-1,3(4)-beta-glucanase produced with *Talaromyces versatilis* IMI 378536 and DSM 26702 (ROVABIO® ADVANCE) for weaned piglets and pigs for fattening (ADISSEO France S.A.S). *EFSA J.***20**, e07251 (2022).
25. Li, Y. et al. Two acidic, thermophilic GH28 polygalacturonases from *Talaromyces leycettanus* JCM 12802 with application potentials for grape juice clarification. *Food Chem.* **237**, 997–1003 (2017).
26. Crotti, L. B. et al. Studies of pectic enzymes produced by *Talaromyces flavus* in submerged and solid substrate cultures. *J. Basic. Microbiol.* **39**, 227–235 (1999).
27. Fernandes, S., Murray, P. G. & Tuohy, M. G. Enzyme systems from the thermophilic fungus *Talaromyces emersonii* for sugar beet bioconversion. *BioResources* **3**, 898–909 (2008).
28. Azzaz, H., Murad, H. & Hassaan, N. Pectinase production optimization for improving dairy animal's diets degradation. *Int. J. Dairy. Sci.* **15**, 54–61 (2020).
29. Sethi, B. K., Nanda, P. K. & Sahoo, S. Enhanced production of pectinase by *Aspergillus terreus* NCFT 4269.10 using banana peels as substrate. *3 Biotech.* **6**, 36 (2016).
30. Grandmontagne, D., Navarro, D., Neugnot-Roux, V., Ladevèze, S. & Berrin, J. G. The secretomes of *Aspergillus japonicus* and *Aspergillus terreus* supplement the Rovabio® enzyme cocktail for the degradation of soybean meal for animal feed. *J. Fungi Basel Switz.***7**, 278 (2021).
31. Bonnin, E., Dolo, E., Le Goff, A. & Thibault, J. F. Characterisation of pectin subunits released by an optimised combination of enzymes. *Carbohydr. Res.* **337**, 1687–1696 (2002).
32. De Vries, R. P., Kester, H. C. M., Poulsen, C. H., Benen, J. A. E. & Visser, J. Synergy between enzymes from *Aspergillus* involved in the degradation of plant cell wall polysaccharides. *Carbohydr. Res.* **327**, 401–410 (2000).
33. Plouhinec, L. et al. A time-course analysis of *Aspergillus terreus* secretomes reveals the importance of pectin-degrading enzymes to increase the digestibility of soybean meal. *Appl. Environ. Microbiol.* e02153-23 https://doi.org/10.1128/aem.02153-23 (2024).
34. Huisman, M. M. H., Schols, H. A. & Voragen, A. G. J. Enzymatic degradation of cell wall polysaccharides from soybean meal. *Carbohydr. Polym.* **38**, 299–307 (1999).
35. Abramson, J. et al. Accurate structure prediction of biomolecular interactions with AlphaFold 3. *Nature* **630**, 493–500 (2024).
36. Meyer, A. S., Rosgaard, L. & Sørensen, H. R. The minimal enzyme cocktail concept for biomass processing. *J. Cereal Sci.* **50**, 337–344 (2009).
37. Paës, G. et al. Tracking of enzymatic biomass deconstruction by fungal secretomes highlights markers of lignocellulose recalcitrance. *Biotechnol. Biofuels.* **12**, 76 (2019).
38. Couturier, M. et al. Post-genomic analyses of fungal lignocellulosic biomass degradation reveal the unexpected potential of the plant pathogen *Ustilago maydis*. *BMC Genom.* **13**, 57 (2012).

39. Bonnin, E. et al. Mobility of pectin methylesterase in pectin/cellulose gels is enhanced by the presence of cellulose and by its catalytic capacity. *Sci. Rep.* **9**, 12551 (2019).
40. Kaczmarska, A., Pieczywek, P. M., Cybulska, J. & Zdunek, A. Effect of enzymatic modification on the structure and rheological properties of diluted alkali-soluble pectin fraction rich in RG-I. *Sci. Rep.* **14**, 11454 (2024).
41. Li, X., Wang, M., Qiao, J. & Huang, H. Computerassisted enzyme-cocktail approach highly improves bioethanol yield. *ACS Sustain. Chem. Eng.* **9**, 14277–14287 (2021).
42. Mardones, W., Callegari, E. & Eyzaguirre, J. Heterologous expression of a *Penicillium purpurogenum* exo-arabinanase in *Pichia pastoris* and its biochemical characterization. *Fungal Biol.* **119**, 1267–1278 (2015).
43. Sakamoto, T. et al. Molecular characterization of a *Penicillium chrysogenum* exo-1,5-alpha-L-arabinanase that is structurally distinct from other arabinan-degrading enzymes. *FEBS Lett.* **560**, 199–204 (2004).
44. Falck, P., Linares-Pastén, J. A., Karlsson, E. N. & Adlercreutz, P. Arabinoxylanase from glycoside hydrolase family 5 is a selective enzyme for production of specific arabinoxylooligosaccharides. *Food Chem.* **242**, 579–584 (2018).
45. Pouvreau, L., Joosten, R., Hinz, S. W. A., Gruppen, H. & Schols, H. A. *Chrysosporium lucknowense* C1 arabinofuranosidases are selective in releasing arabinose from either single or double substituted xylose residues in arabinoxylans. *Enzyme Microb. Technol.* **48**, 397–403 (2011).
46. Lagaert, S. et al. Substrate specificity of three recombinant α-l-arabinofuranosidases from *Bifidobacterium adolescentis* and their divergent action on arabinoxylan and arabinoxylan oligosaccharides. *Biochem. Biophys. Res. Commun.* **402**, 644–650 (2010).
47. Carapito, R. et al. Molecular basis of arabinobio-hydrolase activity in phytopathogenic fungi: crystal structure and catalytic mechanism of *Fusarium graminearum* GH93 exo-alpha-L-arabinanase. *J. Biol. Chem.* **284**, 12285–12296 (2009).
48. Sun, L. et al. Structural characterization of rhamnogalacturonan domains from *Panax ginseng* C. A. Meyer. *Carbohydr. Polym.* **203**, 119–127 (2019).
49. Nakamura, A., Furuta, H., Maeda, H., Nagamatsu, Y. & Yoshimoto, A. Analysis of structural components and molecular construction of soybean soluble polysaccharides by stepwise enzymatic degradation. *Biosci. Biotechnol. Biochem.* **65**, 2249–2258 (2001).
50. Yu, L. et al. Rhamnogalacturonan I domains from ginseng pectin. *Carbohydr. Polym.* **79**, 811–817 (2010).
51. Shakhmatov, E. G., Makarova, E. N. & Belyy, V. A. Structural studies of biologically active pectin-containing polysaccharides of pomegranate *Punica granatum*. *Int. J. Biol. Macromol.* **122**, 29–36 (2019).
52. Sengkhamparn, N., Verhoef, R., Schols, H. A., Sajjaanantakul, T. & Voragen, A. G. J. Characterisation of cell wall polysaccharides from okra (*Abelmoschus esculentus* (L.) Moench). *Carbohydr. Res.* **344**, 1824–1832 (2009).
53. Shi, H. et al. Structural characterization of a rhamnogalacturonan I domain from ginseng and its inhibitory effect on galectin-3. *Molecules* **22**, 1016 (2017).
54. Demarco, A. & Gibon, V. Overview of the soybean process in the crushing industry. *OCL* **27**, 60 (2020).
55. Kondo, T. et al. Biochemical and structural characterization of a novel 4-O-α-l-rhamnosyl-β-d-glucuronidase from *Fusarium oxysporum*. *FEBS J.* **288**, 4918–4938 (2021).
56. Aquilina, G. et al. Scientific Opinion on Rovabio® Excel (endo-1,3(4)-beta-glucanase and endo-1,4-beta-xylanase) as a feed additive for chickens and turkeys for fattening, laying hens, piglets (weaned) and pigs for fattening, ducks, guinea fowls, quails, geese, pheasants and pigeons. *EFSA J.***11**, 3321 (2013).
57. Lafond, M., Guais, O., Maestracci, M., Bonnin, E. & Giardina, T. Four GH11 xylanases from the xylanolytic fungus *Talaromyces versatilis* act differently on (arabino)xylans. *Appl. Microbiol. Biotechnol.* **98**, 6339–6352 (2014).
58. Woest, C. *Efficacy of Enzymes Produced by Talaromyces versatilis in Releasing Energy and Amino Acids in Broiler Feeds* (University of Pretoria, 2019).
59. Cozannet, P., Kidd, M. T., Neto, M., Geraert, P. A. & R. & Next-generation non-starch polysaccharide-degrading, multi-carbohydrase complex rich in xylanase and arabinofuranosidase to enhance broiler feed digestibility. *Poult. Sci.* **96**, 2743–2750 (2017).
60. Yacoubi, N., Cozannet, P. & Preynat, A. Dietary energy and amino acid enhancement from a multi-enzyme preparation. *J. Appl. Poult. Res.* https://doi.org/10.3382/japr/pfy056 (2018).
61. Guais, O., Llanos, A., Cozannet, P. & Preynat, A. Genomic characterization and gene regulation optimization to further improve an enzymatic mix used as feed additive. *Enzyme Eng. XXIV* (2017).
62. Guais, O. et al. Proteomics analysis of Rovabio™ Excel, a secreted protein cocktail from the filamentous fungus *Penicillium funiculosum* grown under industrial process fermentation. *J. Ind. Microbiol. Biotechnol.* **35**, 1659–1668 (2008).
63. Black, I. M. et al. Acetylation in ionic liquids dramatically increases yield in the glycosyl composition and linkage analysis of insoluble and acidic polysaccharides *Anal. Chem.* **95**, 12851 (2023).
64. Haon, M. et al. Recombinant protein production facility for fungal biomass-degrading enzymes using the yeast *Pichia pastoris*. *Front. Microbiol.* **6**, (2015).
65. Miller, G. L. Use of dinitrosalicylic acid reagent for determination of reducing sugar. *Anal. Chem.* **31**, 426–428 (1959).
66. Navarro, D. et al. Automated assay for screening the enzymatic release of reducing sugars from micronized biomass. *Microb. Cell. Factories*. **9**, 58 (2010).
67. Barnes, W. J. et al. Protocols for isolating and characterizing polysaccharides from plant cell walls: a case study using rhamnogalacturonan-II. *Biotechnol. Biofuels*. **14**, 142 (2021).

Acknowledgements

The PhD fellowship of L.P. was funded by Adisseo® and the Association Nationale Recherche Technologie through the Convention Industrielle de Formation par la Recherche (grant no. 2021/1432). The carbohydrate analyses were supported by the U.S. Department of Energy, Office of Science, Basic Energy Sciences, grant number DE SC0015662 to P. A., at the Complex Carbohydrate Research Center. Substrate preparation was supported by the U.S. Department of Energy, Office of Science, Biological and Environmental Research, Genomic Science Program grant no. DE-SC0023223 to B.U. The authors thank J. Armengaud, M. Kielbasa, G. Miotello and J.-C. Gaillard from ProGénoMix platform (progenomix.fr) at CEA Marcoule for carrying the shotgun proteomic analyses of the fungal secretomes. The authors thank E. Drula from the CAZy team for annotating the proteomes of the strains. Part of the work described was performed using services provided by the 3PE platform (www.platform3pe.com), a member of IBISBA-FR (www.ibisba.fr), the French node of the European research infrastructure, EU-IBISBA (www.ibisba.eu).

Author contributions

L.P. carried out most of the experiments and drafted the manuscript. A.P., M.H. and S.G. contributed to protein production and ionic chromatography. L.Z. isolated pectins from Arabidopsis and soybean meal and I.B. carried out linkage analysis by gas chromatography coupled with mass spectrometry. D.N. contributed to liquid chromatography coupled with mass spectrometry analyses. L.P., P.A., J.-G.B., B.U., and M.L. designed the ex-

periments and interpreted the data. V.N., J.-G.B. and M.L. conceptualized the study. J.-G.B. and M.L. supervised the work. All authors contributed to the writing of the manuscript, reviewed, and approved the final version of the manuscript.

Declarations

Competing interests

The authors declare no competing interests.

Additional information

Supplementary Information The online version contains supplementary material available at https://doi.org/10.1038/s41598-024-83289-4.

Correspondence and requests for materials should be addressed to J.-G.B. or M.L.

Reprints and permissions information is available at www.nature.com/reprints.

Publisher's note Springer Nature remains neutral with regard to jurisdictional claims in published maps and institutional affiliations.